

Spacers in the treatment of hip joint infections: numerical analysis of their durability

Brenda Weiss, Sebastián Vanrell, Marcelo Berli, Sebastián Ubal y José Di Paolo

Grupo Biomecánica Computacional, Facultad de Ingeniería, Universidad Nacional de Entre Ríos. Ruta Provincial 11, km 10, 3100 Oro Verde, Entre Ríos, Argentina

E-mail: bweiss@bioingenieria.edu.ar, srvanrell@conicet.gov.ar

Abstract. Hip spacers are temporary implants having a geometry similar to the femoral component of a hip prosthesis, and they are manufactured with antibiotic-impregnated bone cement. The use of spacers in two stage revisions is the most effective treatment to eradicate infections and to avoid limb shortening. The most frequent complication associated with spacers is fatigue failure, for which doctors recommend patients to stay at rest. In this work, several spacer designs are analyzed in order to determine the feasibility of doing activities like walking, standing up or sitting down while performing the antibiotics treatment. Designs combine both different neck diameters and the presence/absence of an internal, stainless steel reinforcement. By means of computational simulations based on the finite element method, stress fields are calculated for various hip spacer designs under several load and fixing conditions. For this purpose, a 3D model of human femur is generated by processing tomographic images with segmentation techniques and inverse engineering. The results allow us to estimate the life expectancy of each design, by considering the fatigue behavior of the bone cement. Only the introduction of a reinforcement with a proper diameter into the bone cement matrix could assure the integrity of the spacer along the treatment period.

1. Introduction

Total hip replacement is a successful solution to relieve pain and restore hip movement [1]. Despite the success achieved with hip prosthesis, hip arthroplasty could lead to several complications, among which infections are the most feared because available treatments are complex, expensive and not always effective [2, 3].

Currently, the most effective treatment to eradicate the infection involves the extraction of the implant, followed by the administration of antibiotics and then the placement of a new implant after 2-6 months since the extraction surgery. Therefore, the patient must remain at rest and practically incapable to move the affected limb, which leads to leg shortening. In order to overcome these drawbacks, hip spacers are now usually implanted during the time interval between the two surgeries, showing infection healing in more than 93% of the cases [2].

Hip spacers have a geometry similar to the femoral component of metallic prosthesis and are manufactured from antibiotic-impregnated bone cement. While handmade spacers (crafted at the moment of implantation) are sometimes implanted, preformed spacers show less complications [4] and are the only ones to be analyzed in this work. In fact, mechanical failures are considered the most important complication among those associated with spacers.



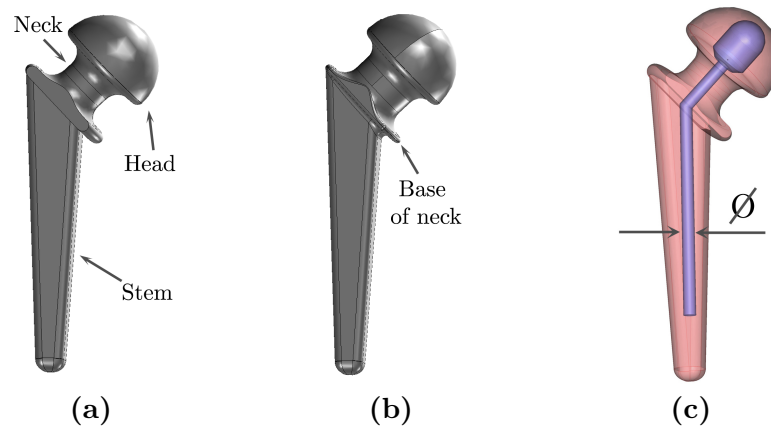


Figure 1. (a) Standard Spacer. (b) Thick Neck Spacer. (c) Standard Spacer reinforced with 316L stainless steel endoskeleton. The bone cement matrix is shown in pink and the metallic endoskeleton is shown in blue.

Therefore, most doctors recommend to patients having an implanted spacer to remain at rest until the following replacement.

The aim of this work is to provide numerical assessment about the basic activities (e.g. walking, standing up or sitting down) that a patient with a hip spacer can do without compromising the integrity of the implant. This objective is driven by the need to improve the quality of life of these patients. Our finite element-based study allow us to evaluate the stresses which develop for several spacer designs and thus predict their lifespan for each of the activities analyzed .

2. Materials and methods

Since bone cement can be considered as a ductile material we choose a failure criterion based on Von Mises stress. The software COMSOL Multiphysics, which is based on finite element analysis, was used to study the stress distribution on spacers.

2.1. Description of spacers

At first, a spacer's geometry design (called *Standard Spacer*, SS_{nR} , see Fig. 1a) was proposed by the *Grupo de Biomateriales para Prótesis* (GBP) from *Facultad de Ingeniería, Universidad de Buenos Aires*; later, as a result of a collaborative work, this design was improved based on our numerical predictions. The first design has a 24 mm-diameter-neck, is entirely built with bone cement and nowadays is implanted in Argentina.

The neck of the spacer presents the highest stresses (as will be seen later) hence a design with a larger (10%) neck diameter, called *Thick Neck Spacer* (TNS_{nR} – Fig. 1b), is proposed. In addition, the incorporation of a 316L stainless steel reinforcement is proposed (Fig. 1c). The diameter of the reinforcement, being a design parameter of this study, is modified throughout the simulations. Due to this reason, the spacer designs simulated are: SS_6 , $SS_{8.4}$ and $SS_{10.2}$ (*Standard Spacer with Reinforcement* of 6 mm, 8.4 mm and 10.2 mm of diameter, respectively), and TNS_6 , $TNS_{8.4}$ and $TNS_{10.2}$ (*Thick Neck Spacer with Reinforcement* of 6 mm, 8.4 mm and 10.2 mm of diameter, respectively)

2.2. Human femur geometric reconstruction

The tomographic images (CT images) employed in this work correspond to the right femur of an adult male (subset of the dataset called *Obelix*, freely available in the *OsiriX-Viewer* repository).

Segmentation of CT images was achieved by combining three techniques implemented in the software *itk-SNAP* [5]: threshold filtering, active contour method (region competition) and manual segmentation. This last step consist of manually filling the space occupied by the medulla (to assure an intimate contact with the spacer) and tweak the sectors with geometric complexity, such as the joint surfaces.

The result is a collection of binary images where the intensity of each pixel codifies whether the corresponding voxel belongs or not to the space occupied by femur. This kind of information is enough to delimit the femur geometry; however, it still is a set of stacked 2D images that can not be entered (as a valid geometry) into the simulation software. Therefore, the outer surface of femur was extracted and represented by an interconnected mesh of triangles that results from employing the marching cubes algorithm, implemented in *itk-SNAP* [5].

Given the irregularity of the resulting surface, a Laplacian smoothing process (low pass filter) was applied to recover the curvature of the actual anatomical surface. This filter does not change the mesh topology (number of nodes and their interconnections), but instead alters the nodes position which define the triangles so that there are no abrupt changes between the orientation of neighboring facets.

While generation of a volumetric model is not required, it is desirable given the advantages that arise at later stages. To obtain that model, which is suitable for being incorporated in a finite element software, we have used a discrete set of irregular parameterized surfaces (like patches), as NURBS surfaces (*non-uniform rational basis spline*, see [6]), to generate a volumetric model by interpolation of a smoothed surface mesh. This procedure was carried out using CAD tools.

The volumetric model of the femur is incorporated into COMSOL Multiphysics as a geometric domain. The aim of this work is to study the stresses that develop on the spacer, which is located in the proximal femur. Hence, in order to reduce computational requirements and simplify the model geometry in a region that is not of interest (condyles), the femur was transversely sectioned at the distal end of the diaphysis.

2.3. Model characteristics

The following assumptions were considered to formulate the physical model:

- Materials are modeled as linear elastic homogeneous solids.
- During a hip arthroplasty the proximal epiphysis is sectioned, thus leaving out almost all cancellous bone. Therefore, the femur model considered in this work is made of cortical bone only. Distal epiphysis is not modeled.
- The human femur can be modeled as an orthotropic solid, whose properties are shown in Table 1. Ashman measured them using ultrasound techniques [7].
- The materials employed to manufacture the hip spacer (both stainless steel and bone cement) can be considered isotropic solids; their mechanical properties were taken from literature: 316L stainless steel ($E = 193 \text{ GPa}$ y $\nu = 0.25$ [8]), bone cement ($E = 1.47 \text{ GPa}$ y $\nu = 0.35$ [9]).
- Materials undergo small deformations, hence these and displacements are linearly related.
- Metal-polymer and polymer-bone interfaces are intimate and perfect, hence there is no sliding, verifying continuity of displacements and stresses there.

2.4. Fixing conditions

Two fixing conditions were compared by applying identical loads to spacers of equal characteristics. The aim of this study was to evaluate advantages or disadvantages of employing a

Table 1. Mechanical properties of cortical femur bone [7], where directions correspond to the coordinate system that is shown in figures 2c and 2d.

Young Modulus		Shear modulus		Poisson ratio	
E_x	12,9 GPa	G_{xy}	4,53 GPa	ν_{xy}	0,376
E_y	13,4 GPa	G_{xz}	5,61 GPa	ν_{xz}	0,222
E_z	20,0 GPa	G_{xy}	6,23 GPa	ν_{yz}	0,235

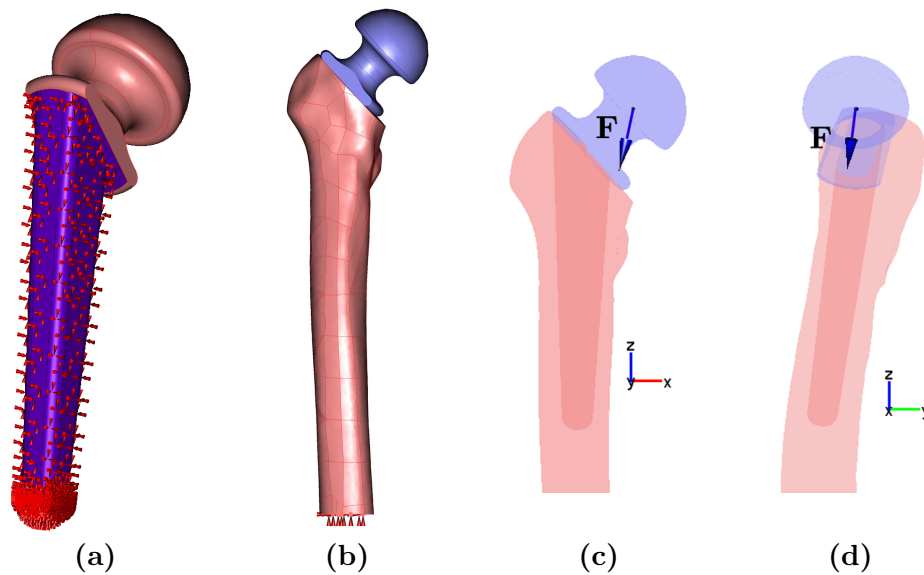


Figure 2. Fixing conditions (null displacement). (a) Fixed-stem. (b) Fixed-femur (at bottom section). Surfaces affected by the condition are marked with red arrows. (c) and (d) Application point of equivalent punctual load \mathbf{F} and its direction.

more complex model (spacer inserted in the femur), which requires more computational resources than simulations of an isolated spacer.

- *Fixed-stem spacer (FS)*: If femur is assumed as a perfectly rigid solid, we can avoid modeling it, by fixing the surface of the spacer that is in contact with the femur—which correspond to the stem—. There, null displacement boundary conditions are considered (Fig. 2a).
- *Fixed-femur spacer (FF)*: Null displacements condition is applied to the distal section of the femur (Fig. 2b), which corresponds to mechanical tests that have been done in other research works [10–12].

2.5. Loading conditions

Although the applied load, as on a healthy femur, is distributed over the spacer's head surface, we consider an equivalent point load \mathbf{F} which is applied on the center of spacer's head (Fig. 2c and 2d). Both the magnitude and direction of \mathbf{F} were determined by Bergmann [13]. For each activity, the value of \mathbf{F} represents the maximum force that appears once per gait cycle.

Simulated activities in this work are normal walking (NW), slow walking (SW), fast walking (FW), up stairs (US), down stairs (DS), stand up (SU) and sit down (SD).

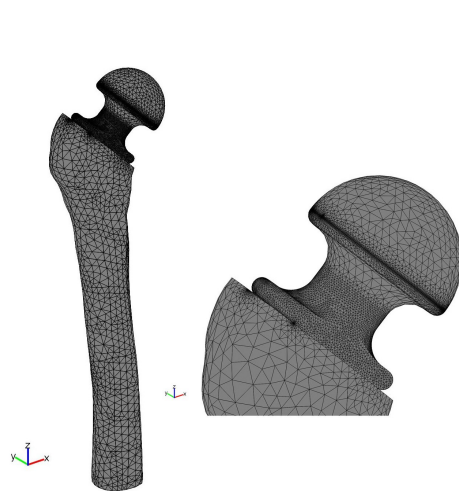


Figure 3. Characteristic element mesh distribution.

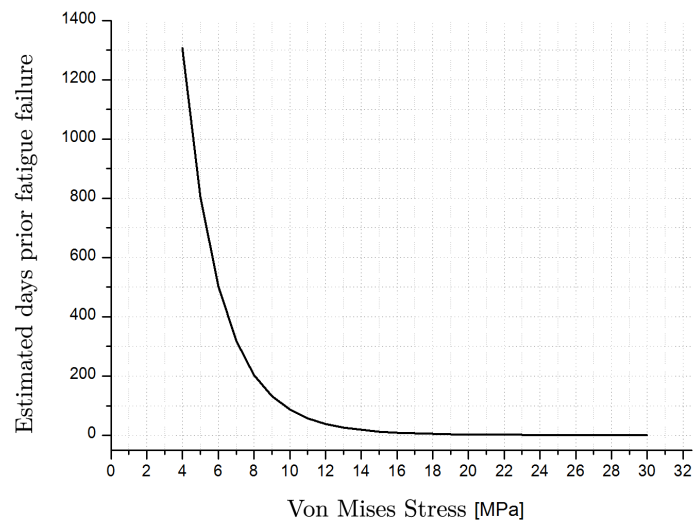


Figure 4. Estimated days prior to fatigue of bone cement as a function of maximum Von Mises stress on this material.

2.6. Solving methodology

The greatest stresses appear on the spacer's neck, so it is important to analyze the mesh influence in this particular zone, specifically on the maximum Von Mises stress developed there. Therefore, a convergence analysis has been carried out by manually modifying parameter h —maximum size of any mesh element— on neck's surfaces. The convergence criterion adopted in this work is that a mesh is fine enough if the change in the maximum Von Mises stress is less than or equal to 2% when halving h in the neck region. This resulted in a maximum element size of 0.001 m.

Meshes are automatically generated by COMSOL Multiphysics (Fig. 3) according to the parameters manually established. These meshes have quadratic Lagrange elements —tetrahedral on volumes and triangular on surfaces— with high resolution (higher quantity of elements per unit volume) in regions where surfaces present significant curvature, and also in those areas where variables present steep gradients. For the solution of the linear system, we use PARDISO (direct) and *Conjugated Gradients* (iterative) solvers.

The maximum values of Von Mises stresses are observed at qualitatively the same regions where fatigue failures are initiated [14]. In addition, the stresses are concentrated on the spacer's neck. As a consequence of these observations, we are interested in the values of the maximum Von Mises stress developed there, as well as in the positions where they appear, since these are the most likely points to result in the spacer's failure. On this stage, results are processed using COMSOL Multiphysics.

The main flaw of spacers is fatigue failure, therefore, considering the results obtained by Lewis [15] and the estimation that a prosthesis implanted in a person of normal activity is subjected to about 1 million annual cycles [10], we built a curve of estimated days prior to cement's fatigue as a function of Von Mises maximum stresses to which this material is subjected (Fig. 4). Then, to estimate the duration of each design, the maximum stresses were *translated* into estimated days prior to cement's fatigue.

3. Results

The maximum Von Mises stresses obtained in all analyzed cases are placed on the neck of spacers. This suggests this region is potentially prone to fatigue failures; indeed this is consistent with

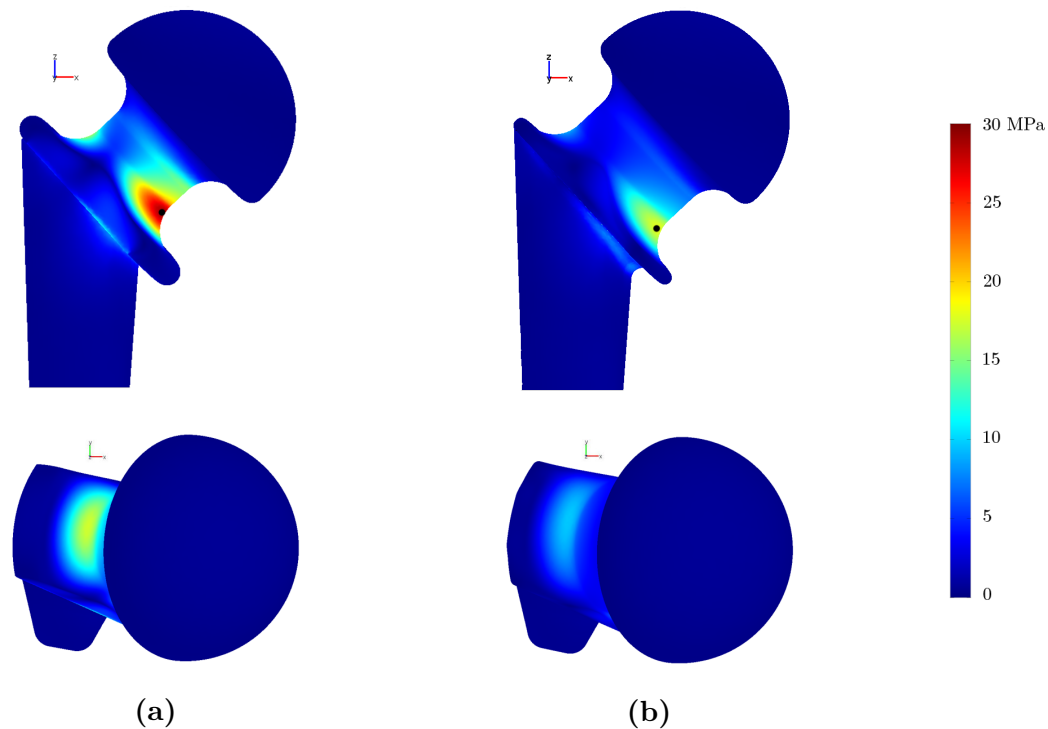


Figure 5. Von Mises stress distribution. A black dot indicates where the maximum Von Mises stress is located. (a) Standard spacer (SS_{nR}). (b) Thick neck spacer (TNS_{nR}).

Table 2. Maximum Von Mises stresses on the neck, cycles prior fatigue and estimated lifetime of non-reinforced spacers. Applied load: 100 kg-patient, normal walking. Fixing condition: fixed-femur.

Spacer	Maximum stress on neck [MPa]	Estimated cycles prior fatigue	Estimated lifetime [days]
SS _{nR}	29,24	1.044	<1 day
TNS _{nR}	18,13	13.151	~5 days

observations from clinical practice [16]. Comparing results for each spacer design and every fixing condition, under identical load direction and magnitude, it is seen that the stress field maintains a similar spatial distribution. As an example, figure 5 shows the stress field for SS_{nR} and TNS_{nR}, under a normal walking of a 100 kg-patient.

3.1. Influence of the diameter of the spacer neck

Table 2 shows the results obtained for implants SS_{nR} and TNS_{nR}, the load corresponding to normal walking of a 100 kg-patient and fixed-femur condition. As can be seen, the maximum Von Mises stress on the neck of both models are significantly different. Under these conditions, the TNS_{nR} presents stresses 38% lower than the SS_{nR}. A similar behavior is observed when comparing SS and TNS reinforced designs under the same loading and fixing conditions. These are reasonable observations since the neck is under bending, thus an increment of neck diameter increases the moment of inertia of the neck's section; therefore this impacts on a stress reduction in this area.

Figure 6a shows the variation of the maximum Von Mises stress on SS_{nR} and TNS_{nR} under

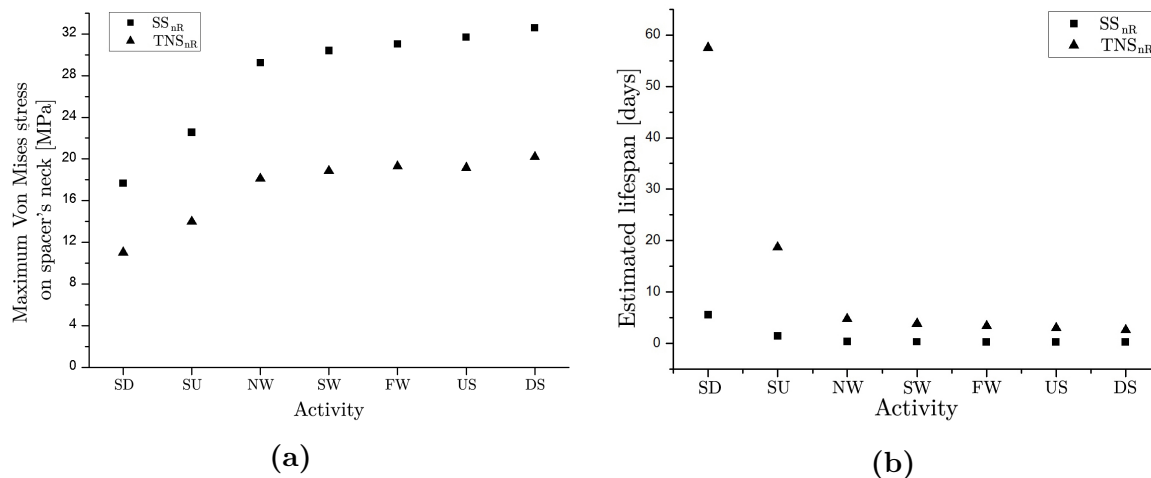


Figure 6. (a) Von Mises maximum stress and (b) estimated lifetime of non-reinforced spacers (SS_{nR} and TNS_{nR}) depending on simulated activities.

routine activities loading conditions: SD, SU, NW, SW, FW, US and DS. Regardless of the activity, the maximum stresses are higher in standard spacers. The highest maximum stresses are observed in FW, US and DS, while the lowest are seen when sitting down or standing up, two essential activities to improve the patient life quality during infection treatment.

Figure 6b is obtained by *translating* stresses shown in figure 6a into estimated duration days. In figure 6b can be seen that most of the activities determine a similar spacer lifetime (<7 days), except when sitting or standing with a TNS_{nR} implanted. The difference observed in the latter cases is accentuated by the non-linearity (exponential) of the curve used to estimate the durability of the spacer (Fig. 4). Thus, it can be noticed that a small stress reduction from values around 14 MPa causes a considerable increase in the estimated days prior fatigue. In addition, these estimations may be affected by the uncertainty of the experimental curve obtained by Lewis [15].

Consequently, we can estimate that a TNS_{nR} could be under normal walking for 5 days, and that SS_{nR} could not even withstand one day (Table 2). Then, none of the designs (SS_{nR} and TNS_{nR}) presents stress values on the bone cement small enough to ensure the spacer integrity during the treatment, when carrying out the analyzed activities.

3.2. Influence of fixing condition

When a TNS_{nR} is implanted in a 100 kg-patient and the two fixation conditions (Fixed-Stem and Fixed-Femur) are compared, figure 7 is obtained. It can be noted that the fixed-femur condition shows stresses $\sim 5\%$ higher than the fixed-stem condition. This trend in the results suggests that the simplest model (FS) could be used to estimate the spacer lifetime, after applying a safety factor to the computed maximum stress. This would allow to employ the FS model, which is considerably less expensive computationally, due to the smaller degrees freedom to be solved for in the model.

3.3. Influence of reinforcement diameter

A metallic reinforcement incorporation significantly decreases maximum Von Mises stresses on the necks of SS_{nR} and TNS_{nR} (Fig. 8). This is reasonable since the stresses that the spacer must withstand are absorbed by the higher stiffness zone: the reinforcement.

For example, incorporating a reinforcement of 6 mm diameter into an TNS (TNS_6) represents

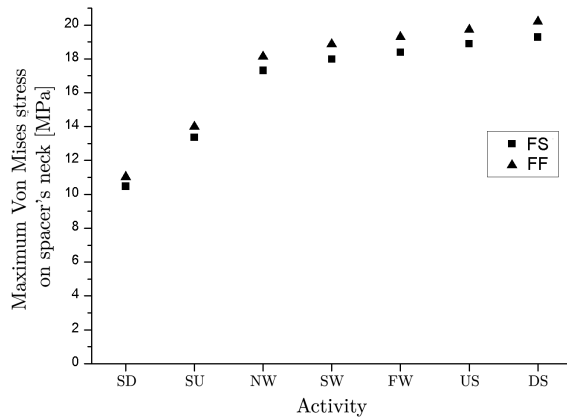


Figure 7. Maximum Von Mises stress on the neck of TNS_{nR} for each activity. FS: Fixed stem. FF: Fixed femur.

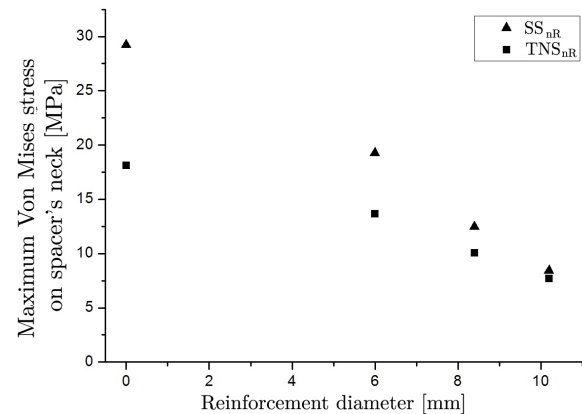


Figure 8. Maximum Von Mises stress on SS and TNS spacer's neck depending on the reinforcement diameter (Non-reinforced spacers are represented with null diameter). Applied load: 100 kg-patient, normal walking.

a 25% reduction of maximum stresses in comparison to TNS_{nR} (non-reinforced). If the reinforcement diameter is increased up to 8.4 mm (TNS_{8.4}) the reduction in stresses is now 45%, whereas it is 58% if the diameter is 10.2 mm (TNS_{10.2}). In terms of lifetime, the incorporation of a 10.2 mm diameter endoskeleton would increase the TNS_{nR} durability—under NW condition—up to approximately 230 days. In the same way, the SS_{nR} lifetime would be 170 days longer when a 10.2 mm diameter reinforcement is incorporated (Table 3).

It should be noted that the influence of neck spacer diameter is significant for non-reinforced spacers—maximum Von Mises stresses for TNS_{nR} are 38% lower than for SS_{nR}—being this not the case for those with a 10.2 mm diameter reinforcement—maximum Von Mises stresses for TNS_{nR} are 9% lower than for SS_{nR}— (Fig. 8).

4. Discussion

Table 3 summarizes the results obtained for 100 kg-patients, showing estimated duration (in days) until failure by fatigue, for different spacer designs and activities. In all the cases considered there, the fixed-femur (FF) condition is employed since the results obtained are more conservatives, given the larger maximum stresses observed under this type of fixation.

Even though some of the simulated designs—those in yellow in Table 3—have an estimated lifetime between 2 and 6 months (i.e. the typical medical treatment interval, see [10]), a durability equal to or larger than 6 months is desirable—results in green in Table 3—in order to assure the integrity of the implant during the treatment.

As indicated in Table 3, spacer TNS_{10.2} is the most promising, since it is the only one that allows the patient to develop all the activities considered in this work, during the whole treatment interval. Designs TNS_{8.4} and SS_{10.2} would also allow performing most of the activities, though for a reduced period.

For simplicity, we considered in this study that the implanted patient possesses a level of activity comparable to that of a normal person (same number of cycles per unit time, same force pattern transferred to the affected hip). Therefore, even though the remaining designs are

Table 3. Estimated durability (in days) of the different spacer designs, subjected to several daily activities (SW, NW, FW, US, DS, SU, SD), when implanted in a 100 kg-patient. Fixed-femur condition. Yellow cells: durability between 2 and 6 months. Green cells: durability equal to or larger than 6 months.

Spacer	SD	SU	NW	SW	FW	US	DS
SS _{nR}	6	1	0	0	0	0	0
SS ₆	47	14	3	3	2	2	2
SS _{8.4}	262	107	33	27	24	21	19
SS _{10.2}	765	399	168	141	130	111	108
TNS _{nR}	58	19	5	4	3	3	3
TNS ₆	189	73	21	17	15	13	12
TNS _{8.4}	493	230	85	71	65	55	52
TNS _{10.2}	969	526	232	199	182	161	155

not expected to attain the desired duration when subjected to normal walk, a reduced set of activities (sitting down, standing up, taking a few steps), would be probably possible without compromising the integrity of the spacer during the full treatment interval.

Some other activities (not simulated here), like walking with reduced support of the body weight on the affected limb (e.g. because of the use of a cane or a walker) would surely benefit from lower maximum stresses and consequently and extended lifetime.

Besides, in order to estimate the life expectancy of the implant, we considered that the whole of the loading cycles correspond to a unique activity. As is well known, activities like going up or down the stairs do not represent a substantial fraction of the daily cycles. A more realistic approach should take into account the distribution of daily activities when estimating the duration of the hip spacer.

5. Conclusions

The results shown in this work, obtained from a model with several simplifications, allowed us to estimate the lifetime of different spacer designs under several loading conditions. A particular design (TNS_{10.2}) meets the strength and durability requirements that enable patients both to complete the antibiotics treatment and to carry out basic daily activities that notoriously improve their quality of life. These results could also provide a guideline for the recommendations given to patients regarding the activities they can perform.

The methodology to reconstruct the geometry of the femur could be easily adapted to the reconstruction of the geometry of many other anatomical structures. Furthermore, additional processing of the tomographic images should allow the extraction of material properties of the tissues, leading to more realistic, complete, patient-specific models.

Acknowledgments

The authors would like to thank CIN (*Consejo Interuniversitario Nacional*) and UNER (*Universidad Nacional de Entre Ríos*) for support provided by the *Stimulus to scientific vocation scholarship* and the *Research initiation scholarship under PID UNER 6103*, respectively.

References

- [1] Pagès E, Iborra J and Cuxart A 2007 *Rehabilitación* **41** 280–9
- [2] García-Sánchez I 2001 *Gaceta Médica de Bilbao* **98** 66–67 ISSN 03044858

- [3] Miltz M and Bühren V 2010 *Der Chirurg; Zeitschrift Für Alle Gebiete Der Operativen Medizen* **81** 310–320 ISSN 1433-0385
- [4] Grassi F, D'Angelo F, Pietri M D and Cherubino P 2005 *Journal of Bone & Joint Surgery, British Volume* **87-B** 256–256 ISSN 1358-992X, 2049-4416
- [5] Yushkevich P A, Piven J, Hazlett H C, Smith R G, Ho S, Gee J C and Gerig G 2006 *NeuroImage* **31** 1116–1128 ISSN 1053-8119
- [6] Piegl L 1991 *IEEE Computer Graphics and Applications* **11** 55–71 ISSN 0272-1716
- [7] Ashman R, Cowin S, Van Buskirk W and Rice J 1984 *Journal of Biomechanics* **17** 349–361 ISSN 0021-9290
- [8] Aalco Metals Ltd 2011 Stainless steel 1.4404 - 316L Product data sheet Aalco Metals Ltd Cobham, Surrey
- [9] Kurtz S, Villarraga M, Zhao K and Edidin A 2005 *Biomaterials* **26** 3699–3712 ISSN 0142-9612
- [10] Thielen T, Maas S, Zuerbes A, Waldmann D, Anagnostakos K and Kelm J 2009 *International Journal of Medical Sciences* **6** 280–286 ISSN 1449-1907
- [11] Schileo E, Taddei F, Malandrino A, Cristofolini L and Viceconti M 2007 *Journal of Biomechanics* **40** 2982–2989 ISSN 0021-9290
- [12] Taddei F, Cristofolini L, Martelli S, Gill H and Viceconti M 2006 *Journal of Biomechanics* **39** 2457–2467 ISSN 0021-9290
- [13] Bergmann G, Deuretzbacher G, Heller M, Graichen F, Rohlmann A, Strauss J and Duda G 2001 *Journal of Biomechanics* **34** 859–871 ISSN 0021-9290
- [14] Hung J P, Chen J H, Chiang H L and Shih-Shyn Wu J 2004 *Computer Methods and Programs in Biomedicine* **76** 103–113 ISSN 0169-2607
- [15] Lewis G and Ed Austin G 1994 *Journal of Applied Biomaterials* **5** 307–314 ISSN 1549-9316
- [16] Jung J, Schmid N V, Kelm J, Schmitt E and Anagnostakos K 2009 *International Journal of Medical Sciences* **6** 265–273 ISSN 1449-1907